24th COBEM - 2017

24th ABCM International Congress of Mechanical Engineering
December 3-8, 2017, Curitiba, PR, Brazil

COBEM-2017-1668
EXPERIMENTAL AND NUMERICAL BUCKLING ANALYSES OF TOW STEERED COMPOSITE PLATES

D.A. Pereira, D. A. Rade
Technological Institute of Aeronautics, Division of Mechanical Engineering, São José dos Campos, SP, Brazil
danielpe@ita.br, rade@ita.br
W.L.N. de Mello, V. L. Reis
Lightweight Structures Laboratory, Institute for Technological Research, São José dos Campos, SP, Brazil
T. A. M. Guimarães
School of Mechanical Engineering, Federal University of Uberlândia, Uberlândia, MG, Brazil

Abstract. *This work presents experimental and numerical buckling analyses of variable stiffness composite laminates (VSCL) with curvilinear fibers manufactured using automated fiber placement. The technique used to manufacture the plies of the laminate is called tow steering, which consists in depositing curvilinear fibers on the ply plane. The composites are made with a prepreg tow of carbon fibers and epoxy resin. Two different types of laminates are used to compare their respective bucking loads, one defined as the baseline, having straight fibers and continuous angles, the other being tow steered with variable angles, both having eight layers. The buckling numerical loads are obtained using finite element analyses. For the experimental analyses, the plates were submitted to compression loads until buckling using an MTS testing system and two different approaches were used to obtain the first buckling mode: the first employed two strain gauges bonded at the center of the plate on each side, and the second used 3D out-of-the plane digital image correlation (DIC). The numerical results showed that VSCL presented 5% higher fundamental buckling load than the unidirectional counterpart, while the experimental results presented an increase of 6.7%. One can conclude that the simulation results were in good agreement with the experimental analyses, and that fiber steering can effectively improve the bucking resistance of composite laminates.*

Keywords: *Automated fiber placement, variable stiffness, composite laminates, buckling, tow steering*

1. INTRODUCTION

It is widely recognized that composite materials, especially fiber-reinforced ones, have enormous potential for many applications. The advantage of these materials is the possibility of designing laminates for specific purposes by changing the relative fiber orientations of the plies to maximize the structural efficiency.

More recently, researchers have been looking for new techniques to design CFRP parts as, for example, the variable stiffness composite laminates (VSCL). One way to obtain the VSCL panels is using curvilinear fibers, which consists in laminates having variable fiber angles in each layer, resulting in stiffness which varies from on point to the other (Ribeiro *et al.*, 2014). This provides the designer with more options to design composite plates considering multiple design goals (Wu *et al.*, 2013).

Buckling and post-buckling of traditionally manufactured laminated plates are relatively well-understood phenomena. The structure may deflect when it is subjected to compression loads, resulting in a loss of rigidity. Buckling is therefore characterized by a sudden out-of-plane deflection of a structural member. This can occur even if the loads in the structure are much smaller than those required to cause failure in the material. It is common knowledge that plates with $\pm 45^o$ fiber lay-ups are suitable for first buckling mode due to their ability to resist the twisting deformations; however, they perform poorly in the post-buckling regime. On the other hand, cross-ply laminates (with 0^o and 90^o fibers with respect to the loading direction of the plate) are adequate in terms of post-buckling behavior due to their ability to resist longitudinal and transverse in-plane extension and perform relatively poorly regarding first mode (Weaver *et al.*, 2009). In this context, VSCL exhibit enormous potential for tailoring stiffness for simultaneous improvement of buckling and post-buckling performance of plates (Dodwell *et al.*, 2016). Wu *et al.* (2012) presented a methodology based on the Rayleigh-Ritz method applied to the buckling analysis of general variable stiffness plates; they highlighted the distinct superiority of using variable angle tows for enhancing the buckling response of composite laminates.

Automated fiber placement (AFP) now enables manufacturing more complex geometries, thus opening up a range of designing possibilities of CFRP. As the AFP head is constrained to remain perpendicular to the fiber course, curvilinear fibers are achieved by bending the material in the plane. It should be noted that the quality of the laminate, specifically in

the case of laminates with variable stiffness made with tow steering, is directly related to the control of the manufacturing parameters as fiber deposition and the minimum deposition radius. In this way, it is essential to take into account the intrinsic characteristics of the manufacturing process in any project that involves the use of the composite material. In the specific case of variable stiffness laminates manufactured using the tow steering technique through AFP, the quality of the laminate is essentially related to the radius of curvature used for the deposition and the effects induced by gaps and overlaps of the laminate. Therefore, for radius of curvature less than 500 mm, the tows are increasingly susceptible to manufacturing defects such as misalignment, buckling, wrinkling, gaps and overlaps Dodwell *et al.* (2016).

Due to the recent interest in exploring the exceptional properties of composite materials to optimize both static, dynamic and aeroelastic responses (Guimarães, 2016; Guimaraes *et al.*, 2017), it becomes necessary to develop numerical models and validate them by confrontation with experimental results. Those models must take into account the restrictions of manufacturability and the influence of manufacturing defects.

Therefore, the objective of this study is to evaluate the buckling performance of tow steered rectangular plates manufacture by AFP, accounting for manufacturability constraints, adopting traditional unidirectional composites as baseline for the purpose of comparison. The defects introduced by manufacture limitations were investigated using ultrasound inspection. The laminates were manufactured using the Hexel® prepreg fibers with eight layers; the numerical analysis was performed using Abaqus® and the buckling analysis was performed by compression testing in a 250kN MTS® testing machine.

2. EXPERIMENTAL PROCEDURE

The VSCL were obtained using an automated fiber placement machine, which is settled in the Lightweight Structures Laboratory of Instituto de Pesquisas Tecnológicas do Estado de São Paulo S/A as shown in Figure 1(a) and 1(b). After manufacturing, the inspection of the internal defects was made using the ultrasound technique performed with an automated inspection robot (Figure 1(c)). Finally, the plates were submitted to compression loads until buckling using an MTS testing system as shown in Figure 1(d).

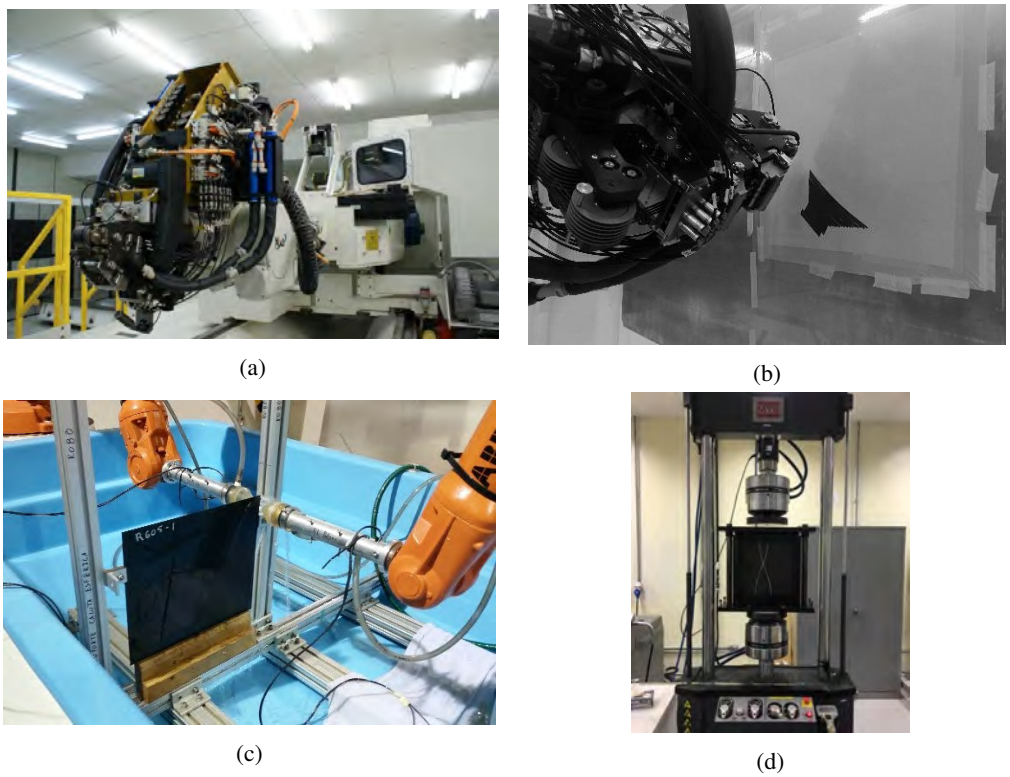

(a) (b) (c) (d)

Figure 1: Experimental devices: (a) automated fiber placement machine; (b) AFP manufacturing process, (c) ultrasound inspection robot and (d) MTS testing machine

3. COMPUTATIONAL PROCEDURE

The AFP equipment has integrated software, which simulates the manufacturing process. Figure 2(a) shows the AFP simulation and Figure 2(b) the curvilinear fibers of the first layer, in which it is possible to see the angles of the fiber starting in 0^o, reaching 45^o and ending in 0^o. Each course of the AFP can have from 4 up to 12 tows. In this work, each

course had 25.4 mm width, being composed of 8 tows of 3.175 width. The first layer is manufactured by eleven courses as shown in the Figure 2(b) (black line).

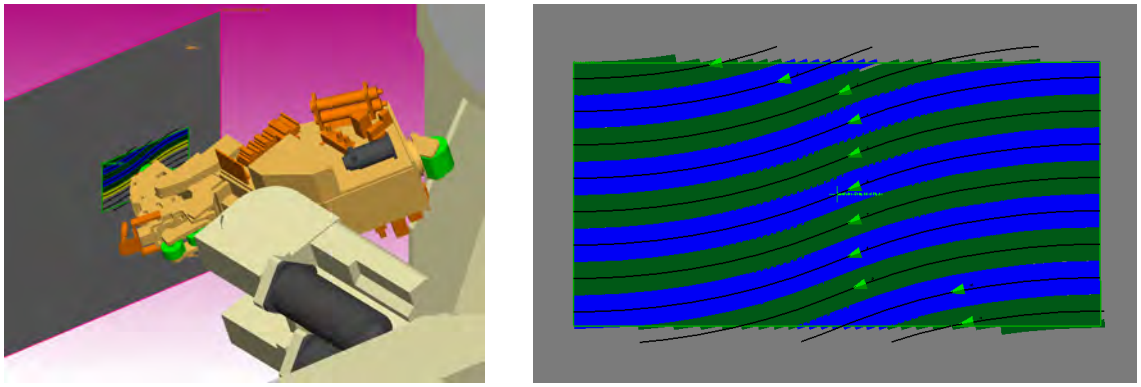

(a) (b)

Figure 2: (a) simulation of the manufacturing process and (b) fiber paths of the first layer.

The simulations were made using Abaqus® finite element software. Each plate was divided in a 25x25 mesh grid, each grid having an orientation angle defined according to Eq. 1 and 2 for the longitudinal and transverse direction, respectively, which have its constants defined in Figure 3.

$$\theta_L(x) = T_1 + 2(T_0 - T_1)\frac{|x|}{a} \tag{1}$$

$$\theta_T(y) = T_1 + 2(T_0 - T_1)\frac{|y|}{b} \tag{2}$$

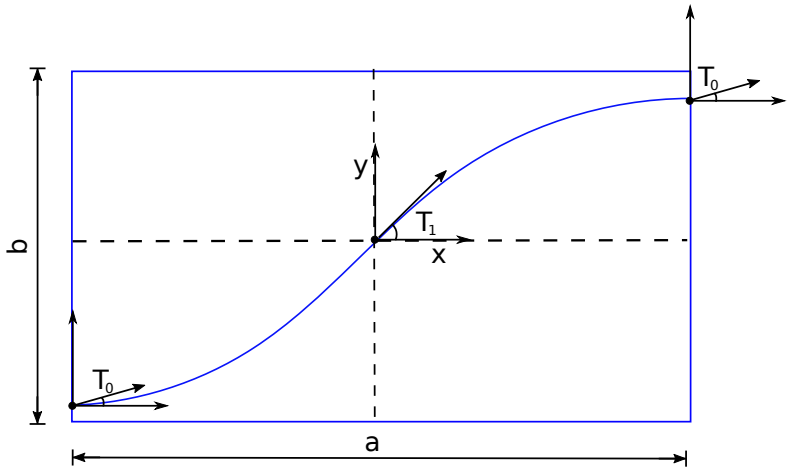

Figure 3: Curvilinear fiber orientation

The baseline plate layers are orientated with $[0/+45/-45/90]_s$. Initially, the idea was to obtain a tow steered plate with a= 400mm and b= 200mm with the orientation $[0 \rightarrow +45 \rightarrow 0/0 \rightarrow -45 \rightarrow 0/90 \rightarrow +45 \rightarrow 90/90 \rightarrow -45 \rightarrow 90]_s$. However, it was found out that the radius of curvature of the third ply was too accentuated, being lower than 605mm, which was adopted as minimum necessary to avoid defects as discussed before. Therefore, the actual orientation of the laminate was chosen as $[0 \rightarrow +45 \rightarrow 0/0 \rightarrow -45 \rightarrow 0/+66 \rightarrow +45 \rightarrow +66/-66 \rightarrow -45 \rightarrow -66]_s$, as depicted in the Figure 4.

4. RESULTS AND DISCUSSION

Figure 5(a) and (c) show the composite plate with conventional and curvilinear fiber orientations, respectively. Figure 5(b) and (d) show the ultrasound results. It is possible to see that as the attenuation of the signal, which indicates the defect density, are similar for both plates, one can conclude that the minimum radius of 605 mm used to manufacture the

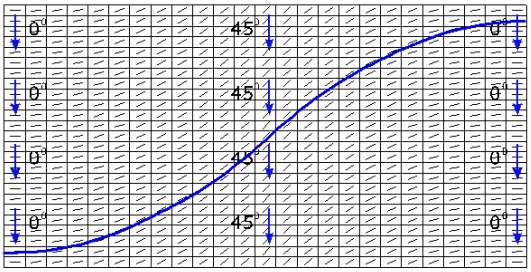

(a) First layer, longitudinal ply $[0 \rightarrow +45 \rightarrow 0]$

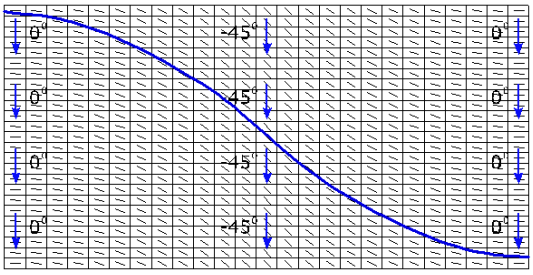

(b) Second layer, longitudinal ply $[0 \rightarrow -45 \rightarrow 0]$

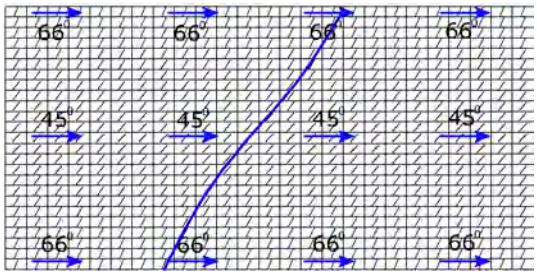

(c) Third layer, transverse ply $[+66 \rightarrow +45 \rightarrow +66]$

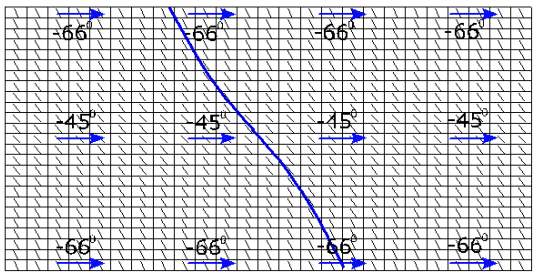

(d) Third layer, transverse ply $[-66 \rightarrow -45 \rightarrow -66]$

Figure 4: Four different layers of the tow steered laminate.

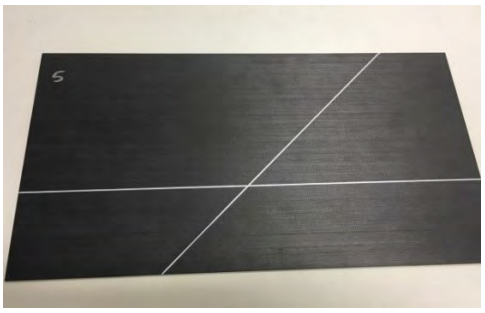

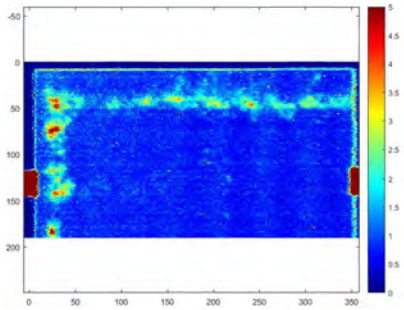

(a)

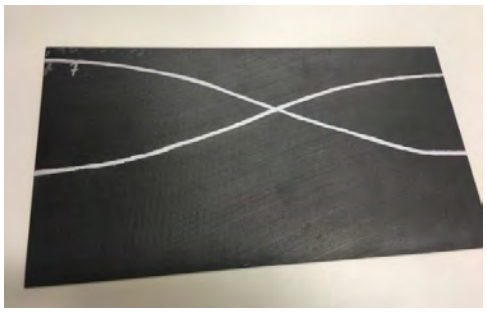

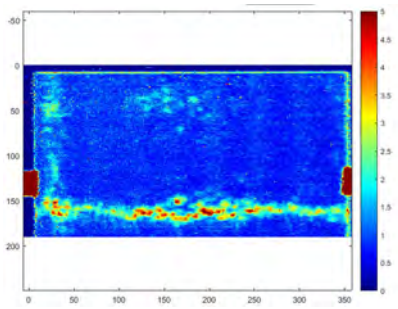

(b) (c)

Figure 5: (a) Baseline plate, (b) ultrasound image for the baseline plate, (c) tow steered plate (d) ultrasound image for the tow steered plate.

tow steered plates was large enough to avoid gaps in the layers. It should be mentioned that the defect concentration in the borders of both laminates are due to the curing process.

Figure 6 shows graphically the numerical analysis of the first and second buckling modes for the baseline and tow steered plates, respectively. Table 1 presents corresponding buckling loads. The plates are subject to axial compression with the boundary conditions being simply supported in the left and right sides and fully clamped in the up and down sides (CSCS), as Figure 7 (a). It was found that, as compared to the baseline plate, the tow steering composite presented an increase of 5% and 8% in both critical loads, respectively. However, the buckling modes are very similar for both plates.

The plates were submitted to compression loads until buckling using an MTS testing system. Two different approaches were used to obtain the first buckling mode: the first used two strain gauges, from HBM ® with gauge factor 2.02, fixed

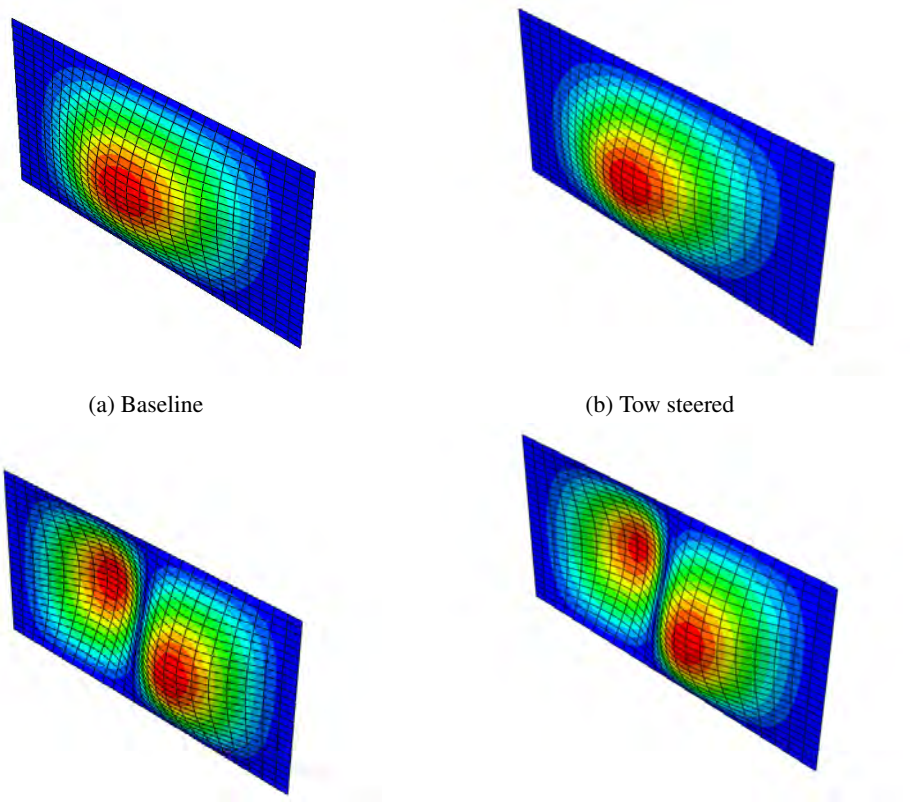

(a) Baseline (b) Tow steered

(c) Baseline (d) Tow steered

Figure 6: (a) and(c) first and second buckling modes for the baseline plate, respectively; (b) and (d) first and second buckling modes for the variable stiffness plate , respectively.

Table 1: Comparison between buckling loads of conventional and tow steered composite plates.

Modes	**Baseline**	**Tow steered**	**Gain %**
First mode	3.83 kN	4.03 kN	5.2
Second mode	4.56 kN	4.94 kN	8.3

at the center of the plate on each side (Figure 7 (a)), and the second used a system of 3D out-of-the plane digital image correlation (DIC) (see Figure 7 (b)), which was made in a cooperation with the Vision Dynamics, which is a subdivision of the LynxUS Inc. group that provides technical services in digital image correlation (VisionDynamics, 2017).

Figure 8 (a) and (b) present the results of load versus strain for the baseline and tow steered plates, respectively. It can be seen that the load increases proportionally with the strain of outputs from bak-to-back strain gauges, A and B, on opposite surfaces at the center of the plate, until approximately 2.5 kN. In the case of buckling the strain indicates its initiation by computing the slope of the vertical curve, as one can see in the Figure 8. This method is called "strain reversal method " (Hu *et al.*, 1946), in which the critical stress is defined as the stress at which the extreme-fiber strain on the convex side of the buckle crest stops increasing and starts decreasing. Therefore, the buckling of the baseline plate occurs when the load is 2.95 kN, while the first mode of the tow steered plate occurs at 3.13 kN, showing an increase of 6.2 %. However, the plate continues to support additional loading in the post-buckling range as the strain continues to increase until the highest loads sustained in this work, which are 8.1 kN and 9.2 kN for the baseline and tow steered plates, respectively.

Figure 9 shows the results obtained by digital image correlation for the conventional plate. It is observed that the maximum out-of-plane displacement was 2.9 mm for an applied force of 8.1 kN (post-buckling regime). Figure 10 shows the DIC picture for the tow steered plate when the compression load is 9.2 kN; for this load, the maximum out-of-plane displacement is 4.06 mm. The out-of-plane displacement of the first buckling mode happened in the opposite direction for both plates due snap through.

Figure 11 (a) and (b) show the out-of-plane displacements **w** of four different loading conditions for the conventional and tow steered plates, respectively, obtained through the DIC for the points on the lines shown in Figures 9 and 10. The results confirm that buckling occurs under the load of 2.95 kN and 3.13 kN for each plate, as represented by the red lines.

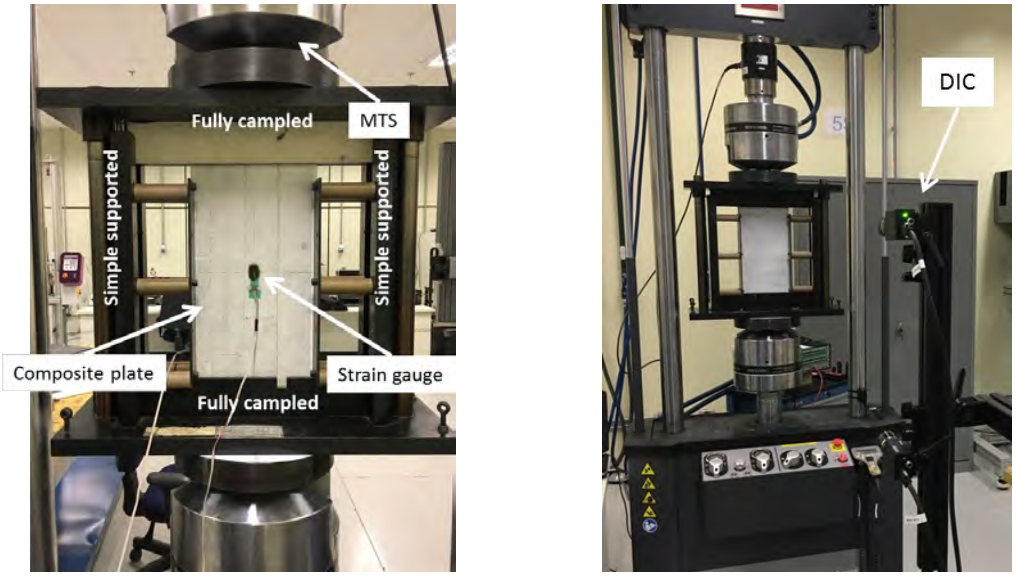

(a) (b)

Figure 7: Experimental test-rig to measure the first buckling load (a) using strain gauges and (b) using digital image correlation.

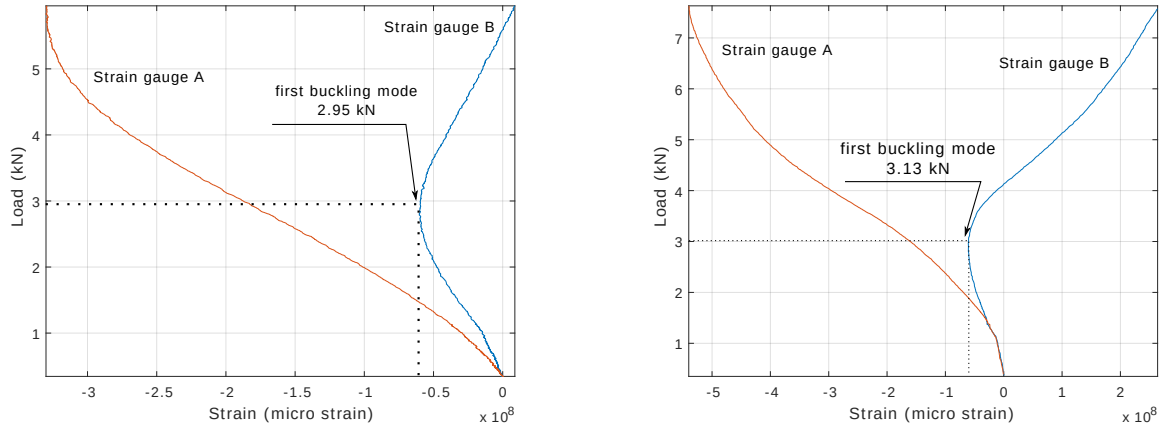

(a) Baseline (b) Tow steered

Figure 8: Experimental curves of the stress and strain measurements of the (a) baseline (buckling happened at 2.95 kN) and (b) tow steered plates (buckling happened at 3.13 kN).

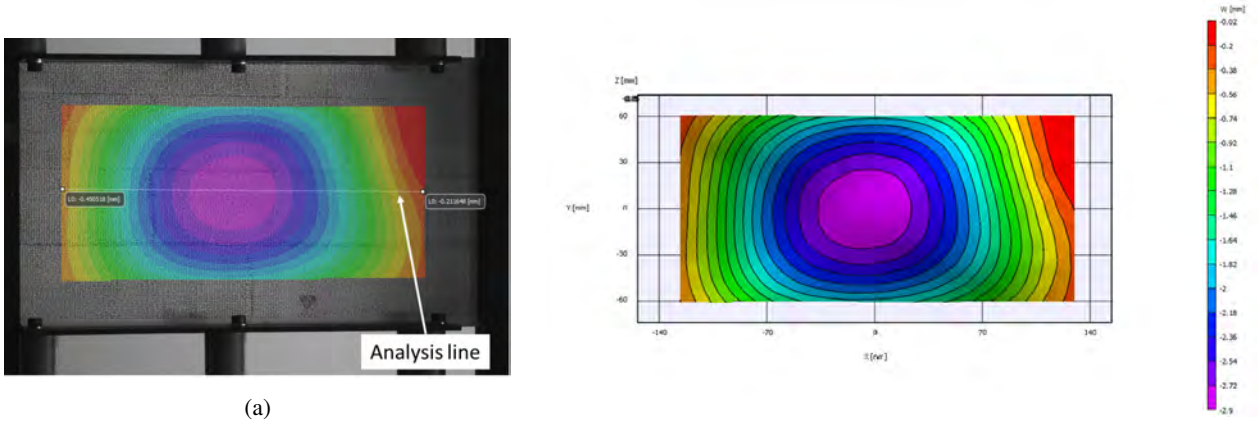

(a) (b)

Figure 9: Digital image correlation of the conventional plate when the load is 8.1 kN.

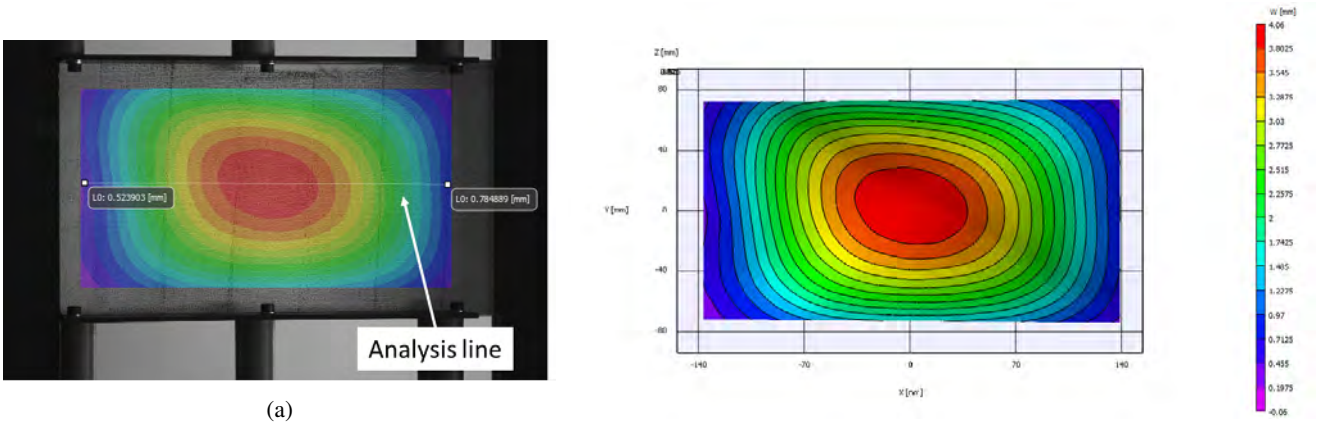

(a) (b)

Figure 10: Digital image correlation of the tow steered plate when the load is 9.2 kN.

It is important to highlight that the midline to measure the out-of-plane displacement does not reach the plate borders. For this reason, the displacements in the extreme of x-axis are not zero.

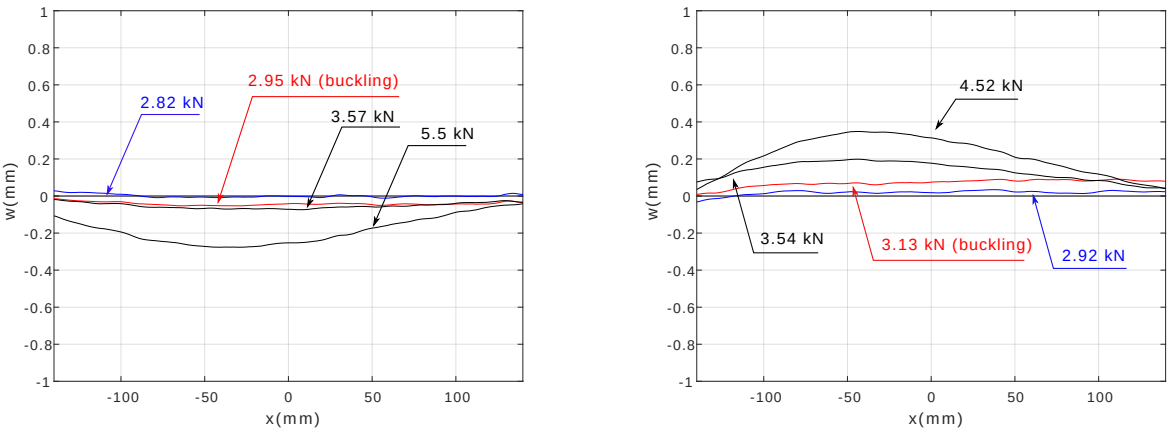

(a) Baseline (b) Tow steered

Figure 11: Out-of-plane displacements obtained by digital image correlation for (a) baseline and (b) variable stiffness plate.

Table 2 shows a comparison between experimental and numerical results. The conventional plate presented a difference of 29 % between the numerical and experimental results, while the plate with tow steered presented a deviation equal to 28 %. These discrepancies are believed to be due to the geometry imperfection and non ideal boundary conditions. As previously mentioned, both numerical and computational results showed an increase of 6.2 % and 5.2 % of the buckling loads when the tow steering technique was used to obtain a plate with variable stiffness.

Table 2: Comparison between numerical and experimental results for conventional and tow steered composite plates for the first buckling load.

Analysis	**Baseline**	**Tow steered**	**Gain**
Experimental	2.95 kN	3.133 kN	6.2 %
Numerical	3.82 kN	4.03 kN	5.2 %
Variation	29%	28%	

5. CONCLUSIONS

This paper presents numerical and experimental buckling analyses of conventional and tow steered composite laminates. The numerical results show that the tow steered plates presented a buckling load increase of 5% and 8% for the

first and second mode, respectively. The experimental results show an increase of 6.2% for the first buckling mode. The difference between numerical and experimental results are approximately 30%. The main highlights of the presented work are: production of composite plates with automated fiber placement using the tow steering technique considering manufacturing constraints, ultrasound analysis to investigate defects caused by gaps and overlaps, use of strain gauges and digital image correlation for determining critical buckling load, and finally, the experimental and numerical assessment of effectiveness tow steering in improving buckling resistance.

6. ACKNOWLEDGEMENTS

This work was supported by Fundação de Apoio ao Instituto de Pesquisas Tecnológicas- FIPT. The author Daniel Pereira acknowledges the financial support of the Brazilian Research Agency CNPq (grant no. 145439/2015-1). D. A. Rade is grateful to CNPq (Projects 442238/2013-3 and 310633/2013-3) and FAPESP (Project 2015/20363-6) for the financial support to his research work. The authors also thanks the Vision Dynamics for helping in the DIC analysis.

7. REFERENCES

Dodwell, T.J., Butler, R. and Rhead, A.T., 2016. "Optimum fiber steering of composite plates for buckling and manufacturability". *AIAA Journal*, Vol. 54:3, pp. 1146–1149.

Guimaraes, T.A., Castro, S.G., Rade, D.A. and Cesnik, C.E., 2017. "Panel flutter analysis and optimization of composite tow steered plates". In *58th AIAA/ASCE/AHS/ASC Structures, Structural Dynamics, and Materials Conference*. p. 1118.

Guimarães, T.A.M., 2016. *Contribuição ao estudo do comportamento dinâmico e aeroelástico de laminados compósitos de rigidez variável*. Ph.D. thesis, Universidade Federal de Uberlândia.

Hu, P.C., Lundquist, E.E. and Batdorf, S., 1946. "Effect of small deviations from flatness on effective width and buckling of plates in compression".

Ribeiro, P., Akhavan, H., Teter, A. and Warmiński, J., 2014. "A review on the mechanical behaviour of curvilinear fibre composite laminated panels". *Journal of Composite Materials*, Vol. 48, No. 22, pp. 2761–2777.

VisionDynamics, 2017. "Digital image correlation & high speed imaging". URL `http://www.visiondynamics.com.br`.

Weaver, P.M., Potter, K.D., Hazra, K., Saverymuthapulle, M.A. and Hawthorne, M.T., 2009. "Buckling of variable angle tow plates: from concept to experiment". In *Proc. of the 50th AIAA/ASME/ASCE/AHS/ASC Structures, Structural Dynamics, and Materials Conference, Palm Springs, CA, USA*.

Wu, Z., Weaver, P.M. and Raju, G., 2013. "Postbuckling optimisation of variable angle tow composite plates". *Composite Structures*, Vol. 103, pp. 34–42.

Wu, Z., Weaver, P.M., Raju, G. and Kim, B.C., 2012. "Buckling analysis and optimisation of variable angle tow composite plates". *Thin-walled structures*, Vol. 60, pp. 163–172.

8. RESPONSIBILITY NOTICE

The authors are the only responsible for the printed material included in this paper.